USING HIGH-RESOLUTION HAND-HELD RADIOMETERS

TO MEASURE IN-SITU THERMAL RESISTANCE

DOUGLAS M. BURCH AND DONALD F. KRINTZ

BUILDING PHYSICS DIVISION,CENTER FOR
BUILDING TECHNOLOGY, NBS

NATIONAL BUREAU OF STANDARDS INTERAGENCY
REPORT 83-2764

THIS WAS THE ONLY COPY AVAILABLE AT TIME OF
BINDING

IR 85-2164

Using high-resolution hand-held radiometers to measure in-situ thermal resistance

Douglas M. Burch and Donald F. Krintz

Building Physics Division, Center for Building Technology,
National Bureau of Standards, Washington, D.C. 20234

Abstract

A field study was carried out to investigate the accuracy of using high-resolution radiometers to determine the in situ thermal resistance of building components having conventional residential construction. Two different types of radiometers were used to determine the thermal resistances of the walls of six test buildings located at the National Bureau of Standards. These radiometer thermal resistance measurements were compared to reference thermal resistance values determined from steady-state series resistance predictions, time-averaged heat-flow-sensor measurements, and guarded-hot-box measurements.

When measurements were carried out 5 hours after sunset when the outdoor temperature was relatively steady and the heating plant was operated in a typical cyclic fashion, the following results were obtained: for lightweight wood-frame cavity walls, the radiometer procedures were found to distinguish wall thermal resistance 4.4 $h \cdot ft^2 \cdot °F/Btu$ (0.77 $m^2 \cdot K/W$) systematically higher than corresponding reference values. Such a discrimination will permit insulated and uninsulated walls to be distinguished. However, in the case of walls having large heat capacity (e.g., masonry and log), thermal storage effects produced large time lags between the outdoor diurnal temperature variation and the heat-flow response at the inside surface. This phenomenon caused radiometer thermal resistances to deviate substantially from corresponding reference values.

This study recommends that the ANSI/ASHRAE Standard 101-1981 be modified requiring the heating plant to be operated in a typical cyclic fashion instead of being turned off prior to and during radiometer measurements.

Introduction

Radiometers are currently used by building energy auditors to assess the thermal resistance of building components. When used for such a purpose, the heat-flow rate at the inside surface of a building component is measured radiometrically, and the in situ thermal resistance is determined by dividing the temperature difference across the component by the measured in situ heat-flow rate. Such a measurement procedure is attractive because of its simplicity and the speed at which the measurement can be carried out. Furthermore, the method is non-destructive and does not require sensors to be mounted onto the subject surface. However, the procedure has been criticized as being inaccurate.

The National Bureau of Standards previously carried out a laboratory and field study [1] to assess the accuracy of such a procedure using low-resolution (i.e., ± 0.5°F or ± 0.3°C) radiation thermometers*. That study found the procedure be inaccurate because the radiation thermometers did not possess sufficient accuracy to resolve adequately the temperature difference between a subject surface and the ambient air in contact with it and because transient heat flows due to diurnal temperature variations and heating plant operation interfered with the measurements. The surface-to-air temperature difference is usually quite small, particularly for insulated building components. The inability to resolve this temperature difference can largely be overcome by using a high-resolution (± 0.1°F or ± 0.05°C) radiation thermometer.

This report presents the results of a field study to investigate the accuracy of high-resolution radiation thermometers and radiant flux radiometers to determine the in situ thermal resistance of a building component. Using two commercially-available high-resolution radiometers, in situ thermal resistance measurements were carried out on the walls of six test buildings located at the National Bureau of Standards in Gaithersburg, Maryland. These measured in situ thermal resistance values were compared to corresponding reference thermal resistance values determined by steady-state thermal resistance predictions, time-averaged heat-flow-sensor measurements, and guarded-hot-box measurements. This study was sponsored by the Navy Civil Engineering Laboratory located at Port Hueneme, California.

---

* Radiation thermometers are referred to as spot radiometers in the building industry.

Description of test buildings

The six test buildings were 20 ft (6.1 m) wide and 20 ft (6.1 m) long one-room buildings with a 7.5 ft (2.3 m) high ceiling. A photograph of one of the test buildings is given in Figure 1. These buildings had the same floor plan and orientation. They were identical,

Figure 1. Photograph of one of the test buildings

except for the wall construction, which was as follows: No. 1. Insulated lightweight wood frame; No. 2. Uninsulated lightweight wood frame; No. 3. Insulated masonry (outside mass); No. 4. Uninsulated masonry; No. 5. Log; and No. 6. Insulated masonry (inside mass). The interior surfaces of the test buildings were painted with an off-white latex paint. Two double-hung, insulating glass (double pane) windows fitted with storm windows were located on the south-facing walls and two on the north-facing walls. Each test building had a 19.5 ft^2 (1.8 m^2) hollow metal door insulated with perlite on the east wall. Two inch (5.1 cm) thick polystyrene insulation was installed over the slab-on-grade floors. Each test building was equipped with a centrally located 4.1 kW electric forced air heating plant equipped with a 13,000 Btu/h (3,800 W) split vapor-compression conventional residential air conditioning system.

A detailed description of the walls of the test buildings is given in Table 1. The reference thermal resistance values for the walls of the test buildings, determined by three independent methods, are summarized in Table 2.

The steady-state thermal resistance values given in Table 2 were calculated using the series-resistance method as outlined in reference [2]. These predicted steady-state values apply to the portion of the wall between structural members, since this is the region where radiometer thermal resistance measurements were carried out.

The heat-flow-sensor thermal resistance values given in Table 2 were determined as follows: a heat-flow sensor, consisting of 2×2 in (5×5 cm) wide and 1/8 in (0.32 cm) thick wafer containing an embedded thermopile, was spot glued at the center inside wall surface (between structural members). The heat-flow sensor produced a D.C. signal proportional to the instantaneous heat-flow rate passing through the device. The heat-flow sensors were calibrated by exposing them to a known uniform heat flux in a thermal conductivity measuring apparatus. Inside and outside surface thermocouples were installed in the immediate vicinity of the heat-flow sensor. The heat-flow rate (q), inside surface temperature (T_{is}), and outside surface temperature (T_{os}) were recorded at hourly intervals over a 5-day period using a data acquisition system. The overall thermal resistance (R_N) was determined from the following running average relation:

$$R_N = R_i + \frac{\sum_{j=1}^{N} (T_{is}-T_{os})_j}{\sum_{j=1}^{N} q_j} + R_o \qquad (1)$$

where R_i is air film thermal resistance at inside surface, 0.68 h·ft^2·°F/Btu (0.12 m^2·K/W); and
R_o is air film thermal resistance at outside surface, 0.4 h·ft^2·°F/Btu (0.07 m^2·K/W).

Table 1. Construction Details of Walls

No. 1 Insulated Lightweight Wood Frame
0.5-in. gypsum board
0.002-in. polyethylene film
2 x 4 studs placed 16 in. o.c. with R-11 glass-fiber insulation installed between the studs
5/8-in. exterior plywood

No. 2 Uninsulated Lightweight Wood Frame
(same as No. 1, except no insulation)

No. 3 Insulated Masonry (Outside Mass)
0.5-in. gypsum board
0.002-in. polyethylene film
2-in.-thick extruded polystyrene insulation placed between 1-1/2-in.-wide wood furring strips placed 24 in. o.c.
1/4-in. air space
4-in., 2-core, hollow concrete block (105 lb/ft^3)
4-in. face brick

No. 4 Uninsulated Masonry
0.5-in. gypsum board
0.002-in. polyethylene film
3/4-in. air space created by 2 x 3/4 in. furring strips placed 16 in. o.c.
8-in., 2-core, hollow concrete block (105 lb/ft^3)

No. 5 Log
7-in. square lodge-pole-pine logs (butt jointed and caulked at the front and rear joints)

No. 6 Insulated Masonry (Inside Mass)
0.5-in. plaster
8-in., 2-core, hollow concrete block (105 lb/ft^3)
3-1/2-in. perlite insulation in the space between block and face brick
4-in. face brick

Table 2. Thermal Resistances for Walls of Test Buildings

Building	Thermal Resistance*, h·ft^2·°F/Btu		
	Steady-State** Predictions	Heat-Flow-Sensor** Measurements	Guarded-Hot-Box Measurements
1	13.2	12.3	12.2
2	3.2	3.3	3.6
3	14.1	14.8	13.7
4	3.6	4.1	4.6
5	9.8	9.8	10.3
6	13.3	12.1	12.4

* These thermal resistance values include air films with thermal resistances of 0.68 h·ft^2·°F/Btu (0.12 m^2·K/W) at inside surface and 0.4 h·ft^2·°F/Btu (0.070 m^2·K/W) at outside surface.

** Values apply to the center portion of the wall between structural members.

The index j is the hourly time index. Thermal resistances determined using this procedure for the north wall of building no. 5 are plotted in Figure 2.

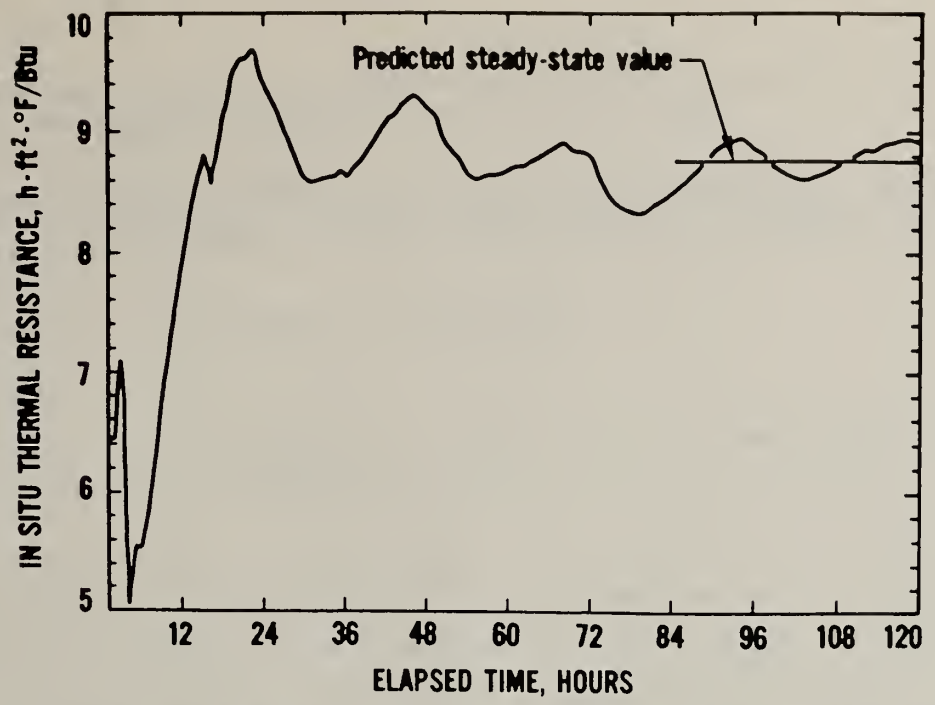

Figure 2. Thermal resistances obtained from heat-flow-sensor measurements for no. 5

The guarded-hot-box thermal resistance values given in Table 2 were determined as follows: Six 6×6 ft (1.8×1.8 m) wall specimens having the same construction as the walls of the test buildings were sent to an independent testing laboratory where they were sandwiched between a hot box maintained at approximately 70°F (21°C) and a cold box maintained at approximately 35°F (1.7°C) and permitted to reach thermal equilibrium. The resulting heat-transfer rate (q) through a 48×32 in (1.2×0.81 m) metering section was measured. The overall steady-state thermal resistance (R) of each test wall was determined from the relation:

$$R = R_i + \frac{T_{is} - T_{os}}{q} + R_o \qquad (2)$$

Here T_{is} and T_{os} are the inside and outside wall surface temperatures, respectively.

Theory and equipment

The apparent thermal resistance (R_a) of an exterior wall is given by the relation:

$$R_a = \frac{T_i - T_o}{q} \qquad (3)$$

where T_i is instantaneous indoor air temperature, °F (°C)
T_o is instantaneous outdoor air temperature, °F (°C)
q is instantaneous heat flow-rate at the inside surface, Btu/h·ft^2 (W/m^2).

Under steady-state conditions, the apparent thermal resistance is equal to the steady-state thermal resistance (R). Two different radiometer procedures for determining the in situ thermal resistance are described below. Both procedures determine the heat-flow rate (q) at the inside wall surface, and compute thermal resistance (R) from Equation 3.

Procedure using a radiation thermometer

In this procedure, the heat-flow rate (q) is determined from the relation:

$$q = h \cdot (T_i - T_{is}) \qquad (4)$$

where h is surface heat-transfer coefficient at the inside wall, Btu/h·ft^2·°F (W/m^2·K); and
T_{is} is inside wall surface temperature, °F (°C).

The surface heat-transfer coefficient (h) is estimated from the relation:

$$h = 4 \cdot E \cdot \sigma \cdot T_s^3 + 0.19 \cdot (T_i - T_{is})^{0.33} \qquad (5)$$

where σ is Stefan-Boltzmann constant, 0.1714×10^{-8} Btu/h·ft^2·R^4 (5.67×10^{-8} W/m^2·K^4);
T_s is average temperature of surrounding surfaces, R(K); and
E is emissivity factor (see Equation 6).

The first and second terms are the radiative and convective components of the surface heat-transfer coefficient, respectively. For the present report, the average temperature of surrounding surfaces (T_s) was taken to be equal to the inside wall surface temperature (T_{is}).

The emissivity factor (E) is estimated from the relation:

$$E = \frac{1}{1/\varepsilon_s + 1/\varepsilon_w - 1} \qquad (6)$$

Here ε_s and ε_w are the surface emissivities for the subject and other room enclosure surfaces, respectively. Taking the emissivities ε_s and ε_w to be 0.9, the emissivity factor (E) is 0.82.

The inside wall surface temperature (T_{is}) was measured by pointing the radiation thermometer shown in Figure 3A at the wall surface and depressing the on-off trigger. The device senses the radiance exiting the surface and is calibrated to read out the apparent radiance temperature on a digital scale to within a resolution of ± 0.1°F (± 0.05°C). The indoor air temperature was estimated by using the radiation thermometer to determine the radiance temperature of a polystyrene board painted with optically-black paint ($\varepsilon_s > 0.98$) placed in front of the subject surface. Manufacturers generally recommend using an object having low heat capacity and high surface emissivity placed in front of the subject surface to determine the inside air temperature.

Procedure using a radiant-flux radiometer

In this procedure, the heat-flow rate (q) is estimated from the manufacturer's equation:

$$q = (1+f_c)\cdot(J_i - J_w) \qquad (7)$$

where f_c is 0.29, factor for the effect of convection (developed by manufacturer);
J_i is incoming radiant flux, Btu/h·ft^2 (W/m^2); and
J_w is outward radiant flux, Btu/h·ft^2 (W/m^2).

The incoming radiant flux (J_i) is sensed by pointing the radiometer shown in Figure 3B at a polystyrene board placed in the center of the room and facing the subject wall surface.* The polystyrene board is painted with optically-black paint ($\varepsilon_s > 0.98$). The incoming radiant flux (J_i) is stored in the device. The radiometer is subsequently pointed at the wall surface, and the outward radiant flux (J_w) is sensed. The heat-flow rate (q) is computed internally utilizing a computer within the device.

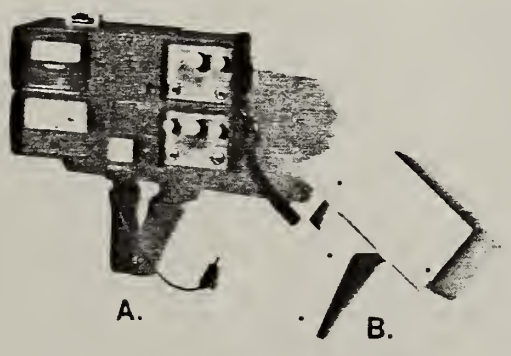

A. Radiation thermometer
B. Radiant-flux radiometer

Figure 3. Photograph of radiometers

* Here it is assumed that the thermal radiation exiting the polystyrene board will essentially equal to the incoming radiation to the subject surface from surrounding surfaces, since $T_s \approx T_i \approx T_{board}$.

Measurements with heating plant turned off

The ANSI/ASHRAE Standard 101-1981 entitled "Application of Infrared Sensing Devices to the Assessment of Building Heat Loss Characteristics" [3] sets forth recommended procedures for carrying out radiometer thermal resistance measurements. This standard recommends that the heating plant be turned off at least 1 hour prior to carrying out radiometer measurements. For the measurements reported in this section, the heating plants of the test buildings were turned off 30 to 60 minutes prior to the radiometer measurements.

Experimental Procedure

Within the six test buildings, radiometer thermal resistance measurements were performed at the center of the north and south walls (between structural members) using the two radiometer procedures previously described. For all radiometer measurements, three instrument readings were taken, and the average of the three readings was reported. The measurements were commenced at about 11:30 p.m. (about 5 hours after sunset) on March 22, 1982. During the measurements, the outdoor temperature varied from 39 (3.9) to 29°F (-1.7°C), and the outdoor wind speed was less than 1 mph (1.6 m/s). Prior to turning off the heating plants, the indoor temperatures of the test buildings were maintained at approximately 68°F (20°C).

Results

Radiometer thermal resistance values are compared with corresponding reference values obtained from time-averaged heat-flow-sensor measurements in Table 3. The heat-flow-sensor values were used as reference values because they were measured in situ at approximately the same locations where the radiometer measurements were carried out. In addition, they agreed with the corresponding values predicted using the steady-state theory and measured using the guarded-hot-box apparatus (see Table 2).

Table 3. Comparison of In Situ Thermal Resistances (Heating Plant Turned Off)

	Thermal Resistance, $h \cdot ft^2 \cdot °F/Btu$			
		Radiation Thermometer		Radiant-Flux Radiometer
Building	Heat-Flow Meter	North Wall	South Wall	North Wall	South Wall
1	12.3	21.9	13.8	10.7	11.4
2	3.3	4.8	4.5	3.3	3.1
3	14.8	61.8	26.1	34.6	14.3
4	4.1	9.1	7.7	6.8	7.6
5	9.8	87.5	22.3	23.5	26.0
6	12.1	95.3	195.	86.5	-38.8

The radiometer thermal resistance values are generally higher than the known values. This trend is more apparent in the heavyweight walls (i.e., nos. 3-6). It is interesting to note that one of the values for building no. 6 is negative.

It was hypothesized that the procedure of turning off the heating plant produced transient heat flows in the walls, thereby causing high apparent thermal resistance measurements. To investigate this possibility, inside wall surface and indoor air temperature thermocouple readings were analyzed. It was found that after the heating plant was turned off, the indoor air temperature of the buildings decayed more rapidly than the inside wall surface temperature due to infiltration and window heat loss. This effect is illustrated for building no. 6 in Figure 4A. During the period from 4:00 to 5:00 a.m., when the heating plant is operating in a typical cyclic fashion, the inside surface and indoor air temperature remained approximately steady, and more important the difference between these temperatures remained approximately constant. After the heating plant was turned off, both the inside surface and indoor air temperatures decreased. However, the indoor air temperature decreased more rapidly than the inside wall surface temperature. The difference between these temperatures approached zero and subsequently became negative. Since the heat-loss rate at the inside wall surface is proportional to this temperature difference, these results indicate that after the heating plant is turned off, the heat-loss rate at the inside wall surface approaches zero and subsequently becomes negative.

Substituting the measured thermocouple measurements given in Figure 4A in Equations 3, 4, and 5, apparent thermal resistance values were computed as a function of time for building no. 6 (see Figure 4B). From 4:00 to 5:00 a.m., the apparent thermal resistance is seen to remain approximately steady. After the heating plant is turned off, the apparent thermal resistance increases rapidly, passes through a discontinuity, and subsequently becomes negative. Similar results were obtained for the other test buildings.

From these measurements, it was concluded that the heating plants of buildings should not be turned off prior to carrying out radiometer thermal resistance measurements. This finding is inconsistent with the ANSI/ASHRAE Standard 101-1981 which recommends that heating

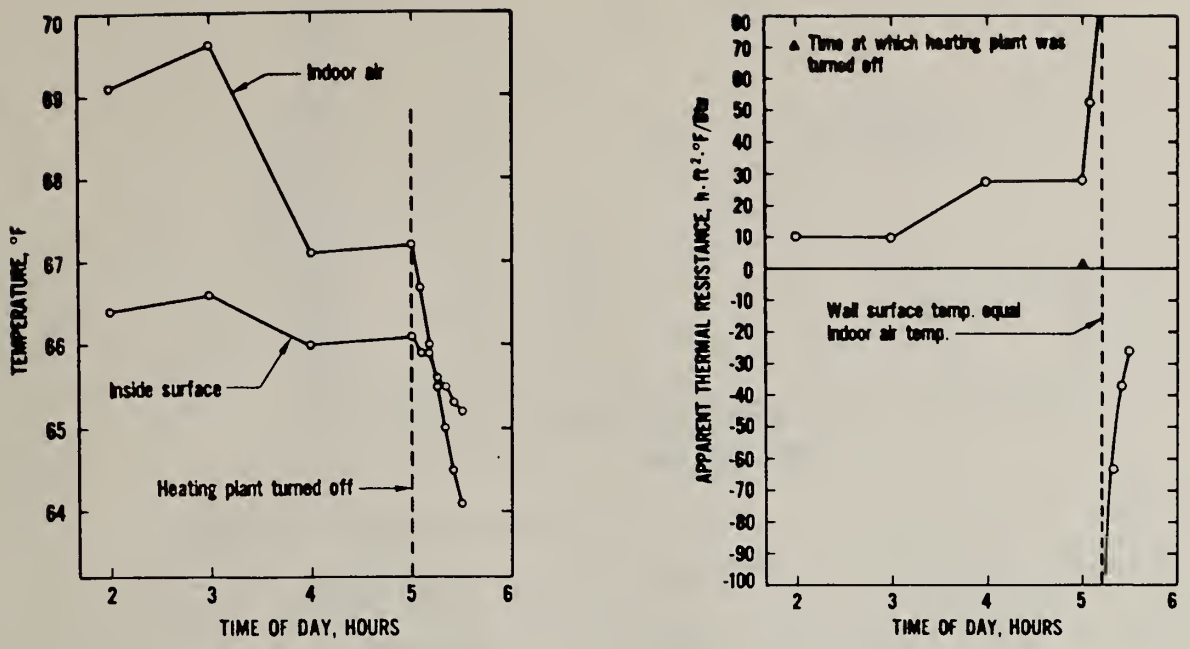

A. Variation in temperature

B. Variation in apparent thermal resistance

Figure 4. Illustration of the effect of turning off heating plant on apparent thermal resistance

plants be turned off prior to radiometer measurements. It is recommended that the ANSI/ ASHRAE Standard 101-1981 be modified to reflect a change in this measurement procedure.

In situ heat-flow rates (q) determined with both types of radiometers were generally found to agree with corresponding coincident values measured with heat-flow sensors.

Measurements with heating plant operated in typical cyclic fashion

For the measurements reported in this section, the heating plants of the test buildings were not turned off prior to carrying out radiometer measurements. The heating plants instead were controlled by their thermostats and operated in a typical cyclic fashion.

Experimental procedure

Within the six test buildings, radiometer thermal resistance measurements were performed at the center (between structural members) of the north wall using only the radiation thermometer. Three separate radiometer readings were taken and averaged for each of the individual measurements reported. The measurements were commenced at about 11:30 p.m. (about 5 hours after sunset) on November 10, 1982. During the measurements, the outdoor temperature varied from 45 (7.2) to 42°F (5.6°C), and the outdoor wind speed was less than 2 mph (3.2 m/s). Outdoor temperatures which occurred prior to radiometer measurements are plotted in Figure 5. Approximately 1 week prior to the measurements, the thermostats of the test buildings were adjusted to maintain an indoor temperature of about 82°F (28°C), in order to provide a large inside-to-outside temperature difference.

Results

Radiometer thermal resistance values are compared with corresponding reference values obtained from time-averaged heat-flow-sensor measurements in Table 4.

Five individual measurements were carried out at randomly different times with respect to the cyclic operation of the heating plant. The mean values given in Table 4 are the arithmetic averages for the five individual measurements. The means for the sets of five radiometer measurements are consistently higher than corresponding reference values. The systematic errors, the difference between the means and reference values, are less than 4.4 $h \cdot ft^2 \cdot F/Btu$ (0.77 $m^2 \cdot K/W$) for the lightweight wood-frame walls (nos. 1 and 2). Such a discrimination will permit the presence or absence of cavity insulation (typically R-11) to be distinguished. However, the systematic errors are considerably larger for the walls having large heat capacity (nos. 3-6).

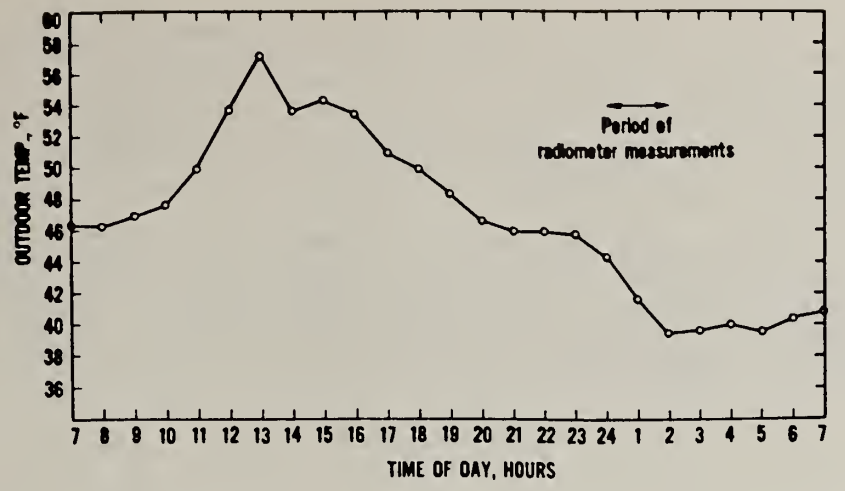

Figure 5. Outdoor temperature variation prior to radiometer measurements

Table 4. Comparison of In Situ Thermal Resistances (Heating Plant Operated in Typical Cyclic Fashion)

	Thermal Resistance, $h \cdot ft^2 \cdot °F/Btu$				
	Radiometer Measurements				
Building	Individual Measurements	Mean	Sample Estimate of Standard Deviation	Reference* Value	Systematic Error**
1	15.2, 18.0, 13.2, 18.7, 18.3	16.7	2.4	12.3	4.4
2	4.4, 4.7, 4.9, 4.6, 4.6	4.6	0.18	3.3	1.3
3	21.8, 23.7, 22.4, 25.9, 26.3	24.0	2.0	14.8	9.2
4	6.5, 7.5, 8.1, 7.8, 8.2	7.6	0.68	4.1	3.5
5	22.2, 23.9, 23.7, 22.2, 21.3	22.7	1.1	9.8	12.9
6	43.6, 30.6, 24.9, 23.1, 32.5	30.9	8.1	12.1	18.8

* Obtained from time-averaged heat flow-sensor measurements (see equation 1)
** Systematic error = mean - reference value

In analyzing the systematic errors, it was found that they appeared to depend upon the "lag times" for the walls. Here "lag time" refers to the elapsed time between the minimum outdoor temperature and the maximum wall heat-loss rate. Lag times for the walls of the six test buildings were determined by analyzing hourly heat-flow-sensor and outdoor temperature measurements over a diurnal period. The systematic errors given in Table 4 are plotted as a function of wall lag times in Figure 6. This plot indicates that a relationship exists between the systematic error and the lag time. The systematic error increases as the lag time increases. As the lag time approaches zero, the systematic error approaches zero.

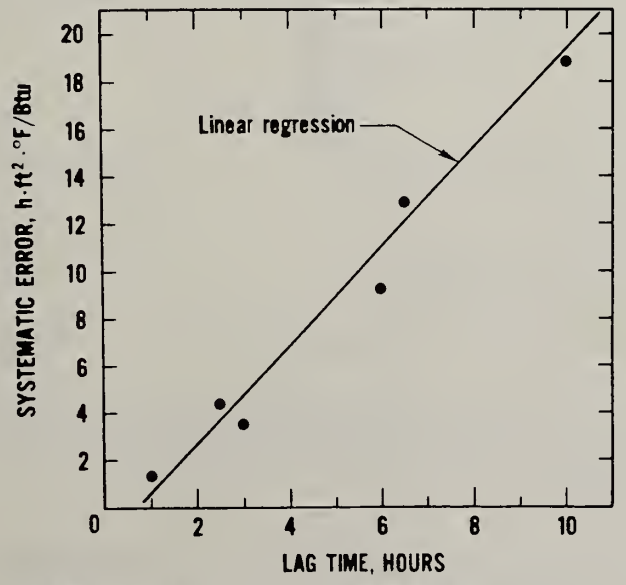

Figure 6. Systematic errors plotted as a function of lag

The diurnal variation in apparent thermal resistance is of considerable interest because such information would provide insight on the effect of thermal storage characteristics on the apparent thermal resistance. Hourly radiometer measurements over a 24-hour period were not available. However, hourly thermocouple temperatures for the inside wall surface, indoor air, and outdoor air were recorded for similar test days. Substituting a diurnal set of hourly thermocouple readings into equations 3, 4, and 5, apparent thermal resistance values were derived for the north wall of building nos. 1 and 5 (see Figure 7).

From Figure 7, it is seen that the apparent thermal resistance for the lightweight wood-frame wall (no. 1) approaches the reference steady-state thermal resistance after 11:00 p.m. However, the apparent thermal resistance for the log wall (no. 5) is considerably greater than steady-state thermal resistance during the night period. This is because the night heat-flow rate for the log wall depends to a greater extent upon previously warm day outdoor temperatures. The log wall never reaches a quasi-steady condition because of its large heat capacity.

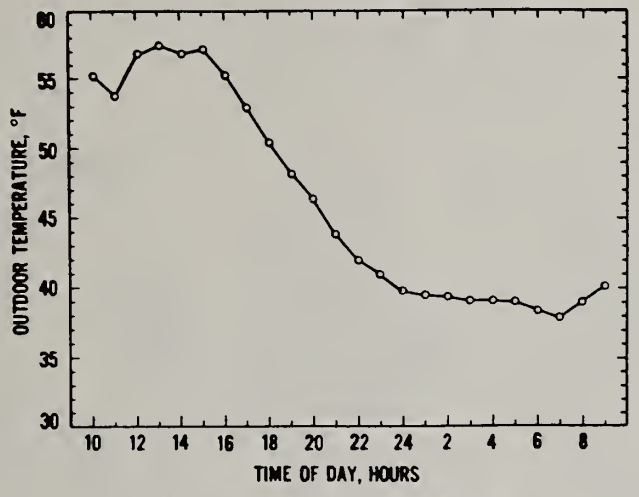

A. Outdoor temperature.

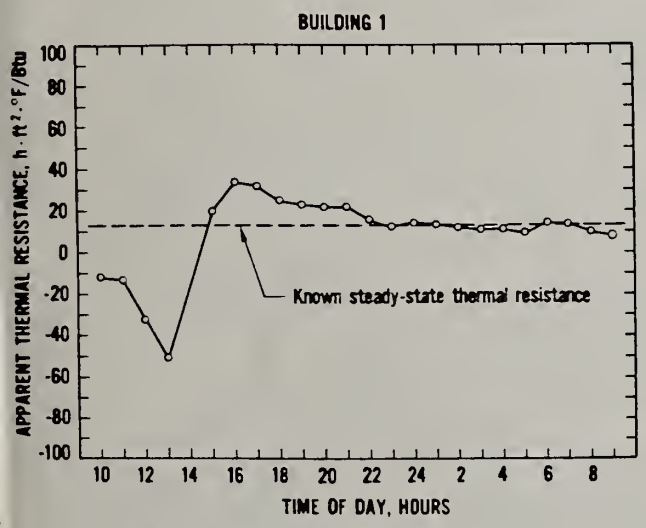

B. Apparent thermal resistance for building no. 1.

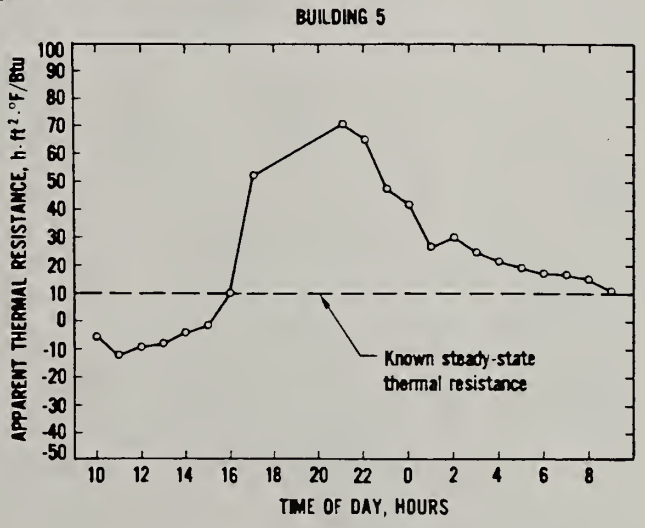

C. Apparent thermal resistance for building no. 5.

Figure 7. Illustration of the variation in apparent thermal resistance during a diurnal period

In Table 4, the sample estimate of standard deviation(s)* provides an estimate for the variability of the individual measurements comprising each data set. Ninety-five percent of the individual measurements are estimated to lie within the range (mean ± 2s). A major

* $s = \sqrt{\frac{\sum_{i=1}^{N} (\bar{y}-y_i)^2}{N-1}}$; where $\bar{y}$ = mean value; y_i = individual measurement; and N = number in set.